scientific reports

Check for updates

OPEN

PDE4B promotes JNK/NLRP3 activation in the nucleus pulposus and mediates intervertebral disc degeneration

Weixing Xu[1,4], Rana Dhar[2,3,4], Kaiyue Li[2,4], Danyang Zheng[1], Minxin He[2], Weiguo Ding[1], Long Xin[1], Bin Xu[1], Yuqing He[2], Qi Peng[2] & Huifang Tang[2,3]✉

Intervertebral disc degeneration disease (IDD) is one of the leading causes of disability, and current therapies are ineffective. Phosphodiesterase 4B (PDE4B) plays essential roles in regulating the activation of the NLRP3 inflammasome. However, whether PDE4B or NLRP3 is involved in the development of IDD is unclear. This study sought to explore the role of PDE4B in IDD pathogenesis by *in vivo* and *in vitro* experiments. This results showed that PDE4B and NLRP3 were significantly upregulated in nucleus pulposus (NP) tissues from IDD-related human patients. Deletion of PDE4B in the NP resulted in downregulated JNK and NLRP3. Aberrant PDE4B expression enhanced the phosphorylation of JNK and NLRP3 expression. Furthermore, genetic ablation of the *pde4b* gene delayed IDD pathogenesis, and PDE4 inhibitor also can reverse the IDD pathogenesis. Our study showed that aberrant PDE4B activation in NP tissues induces pathological changes in IDD, phosphorylation of JNK and NLRP3 are involved in this process, and inhibition of aberrant PDE4B activity is a potential therapeutic strategy for IDD.

Keywords Intervertebral disc degeneration disease, Phosphodiesterase 4B, Nucleus pulposus, NLRP3

Low back pain (LBP) is one of the most common diseases, it not only impacts patients' lives but also causes them to become incapacitated and impose a heavy financial burden on their families and society[1]. Intervertebral disc degeneration (IDD) is one of the most common causes of low back and leg pain, and studies have shown that many factors, such as age, genetics, nutrition, metabolism, infection, and biomechanics, are associated with the incidence of IDD[2,3]. Current therapies for IDD include conservative, interventional, biological, and surgical treatments; although they can achieve good clinical efficacy, they can cause various complications, such as adjacent spondylosis and fusion disease[4]. Moreover, these treatments neither delay the degeneration of intervertebral discs nor regenerate and repair degenerative intervertebral discs. Therefore, an in-depth study of the pathogenesis of IDD is highly important for delaying and preventing IDD.

Several studies have shown that the caspase-1-mediated pyroptosis pathway plays a crucial role in IDD[5–7]. Chen et al. first reported that the expression of NLRP3, Caspase-1, and IL-1β was significantly increased in the intervertebral disc tissue of IDD patients, indicating a positive correlation between NLRP3 activation and the severity of IDD. They also found that IL-1β promotes the expression of NLRP3 through the NF-κB pathway *via* a positive feedback regulatory loop[7]. Sun Y et al. reported that stress can activate NLRP3 through the Ca^{2+}/NF-κB pathway and subsequently promote IL-1β generation, suggesting that stress may also promote the onset of IDD by activating NLRP3[8]. In addition, a recent study showed that *propionibacterium acnes* may be a pathogenic factor for IDD. In nucleus pulposus(NP) tissues infected with *propionibacterium acnes*, the number of NLRP3 positive cells increased sharply[9,10]. These studies suggested that the NLRP3 inflammasome-mediated pyroptosis pathway is an important feature of nucleus pulposus degeneration. However, the underlying molecular mechanism has not been fully elucidated.

[1]Department of Orthopedics, Tongde Hospital of Zhejiang Province, Hangzhou 310012, Zhejiang, China. [2]Department of Pharmacology, School of Basic Medical Sciences, Zhejiang University, Hangzhou 310058, Zhejiang, China. [3]Clinical Laboratory, Sir Run Run Shaw Hospital, Key Laboratory of Precision Medicine in Diagnosis and Monitoring Research of Zhejiang Province, Zhejiang University School of Medicine, Hangzhou 310016, Zhejiang, China. [4]These authors contributed equally to this work: Weixing Xu, Rana Dhar and Kaiyue Li. ✉email: tanghuifang@zju.edu.cn

Phosphodiesterase-4 (PDE4) hydrolyzes the second messenger cyclic adenosine monophosphate (cAMP) in the cell, thereby terminating the biochemical effects of cAMP. PDE4 four subtypes (A, B, C, and D) are encoded by four genes[11]. PDE4B is a subtype of PDE4 expressed mainly in immune cells and the central nervous system and plays an important role in inflammation, the immune response, and tumors[12]. Previous studies suggested that PDE4B is involved in the pathological process of inflammatory and fibrotic damage[13,14]. High expression of PDE4B was found in mouse models of spinal cord injury[15]. Meanwhile, circPDE4B is reportedly downregulated in osteoarthritis (OA) tissues and regulates chondrocyte cell viability and extracellular matrix metabolism[16]. PDE4B is the parental gene of circPDE4B, PDE4B inhibition may be also involved in the chondrocytes of NP tissue, but at present, there are no reports on the correlation between PDE4B and IDD.

The c-Jun N-terminal kinase (JNK) signaling pathway is closely related to the regulation of pyroptosis. Das's studies have shown that in disc degeneration, an imbalance between proinflammatory and anti-inflammatory molecules activates the JNK pathway and induces apoptosis in NPCs, while JNK-specific inhibitors can significantly inhibit the expression of MMP-3 mediated by TNF-α and IL-1β, thereby alleviating the degradation of the extra-NPC matrix[17]. However, the mechanism through which the JNK/NLRP3 signaling pathway affects the pathogenesis of IDD has still been poorly studied.

In this study, we comprehensively analyzed the changes in and correlations between PDE4B, JNK, NLRP3 and IDD through the use of clinical nucleus pulposus tissue samples, human NP cells, and PDE4B knockout mice and revealed that PDE4B induces pyroptosis in NP cells and promotes the occurrence and progression of IDD. Finally, we validated the efficacy of treatments targeting PDE4 via the PDE4 inhibitor roflumilast in a needle puncture-induced IDD rat model, identifying a new therapeutic strategy for IDD.

Methods

Patient nucleus pulposus (NP) samples

Human NP samples were obtained from 12 male patients (mean age 47.9 ± 16.3 years) who were diagnosed with lumbar disc herniation and underwent nucleus pulposus resection. The MRI-based Pfirrmann grading system was used to assess the degenerative grade of the NP specimens. Grade II ($n = 3$), Grade III ($n = 3$), Grade IV ($n = 3$), and Grade V ($n = 3$) NP samples were subjected to WB and ELISA.

Human NP cells culture and treatment

Primary human NP cells were obtained from Procell (Wuhan, China). The cells were cultured at 1×10^5 cells/ml in an atmosphere of 5% CO2 and 95% humidity at 37 °C with complete human disc nucleus pulposus cell medium (CM-H097, Procell, Wuhan, China). The cells were passaged using trypsin/ethylene diamine tetraacetic acid (EDTA) after they reached 90% confluence. After digestion, the cells were seeded at a density of 10^4 cells/cm^2. Cells were continuously passaged for 8 generations, and cells from 3 to 8 generations were used for the experiments.

For cell transfection, NP cells were seeded at a density of 2×10^5 cells/well in 6-well plates. Later, the cells were transfected and co-transfected with the vector control pIRES2-EGFP, the pIRES2-EGFP-PDE4B plasmid, or PDE4B siRNA for 24 h. After 24 h, LPS (10 ng/ml) for 1 h and 10 μM nigericin were added for another 1 h.

Animals

The *pde4b*$^{+/-}$ B6 mice (B6 129P2-*Pde4b*<tm1Dgen>/H, no: EM: 02364) were purchased from the European Mouse Mutant Archive (EMMA). PDE4B knockout mice (*pde4b*$^{-/-}$) and their wild-type littermates (*pde4b*$^{+/+}$) were generated by mating heterozygous mice aged between 8 and 12 weeks. Mice were housed in the Experimental Animal Center of Zhejiang University under standard conditions (23 ± 2 °C, 55 ± 5% humidity, and 12 –12 h light/dark cycle). Twelve-week-old male *pde4b*$^{-/-}$ mice and *pde4b*$^{+/+}$ mice were used in those experiments.

Sprague–Dawley rats (8 weeks old, male) were purchased from the Experimental Animal Center of Zhejiang University (Hangzhou, China) and housed at the Experimental Animal Center of Zhejiang University under standard conditions (23 ± 2 °C, 55 ± 5% humidity, and 12 –12 h light/dark cycle). The rats were randomly divided into 3 groups: the normal group, the IDD model group, and the roflumilast (5 mg/kg, NB1739-1, Meilun, Dalian, China) + IDD model group ($n = 5$ per group).

The study is in accordance with ARRIVE guidelines (https://arriveguidelines.org). All animal procedures were approved by the Animal Ethics Committee of Zhejiang University.

IDD animal model preparation

A mouse IDD model was established in the coccygeal vertebra through a needle puncture. Briefly, after general anesthesia with 2.5% Avertine (20 ml/kg, ip), coccygeal discs were punctured in the areas between the 4th and 7th coccygeal vertebrae (Co4–Co7), using a 26-gauge sterile syringe needle from the dorsal side for 30 s. To ensure degeneration, the needle was passed through the nucleus pulposus (NP) tissue and the bilateral annulus fibrosus (AF), and the needle was rotated in the axial direction by 180° and held for 10 s. To fix the position of the puncture point, an X-ray system (Philips Allura Xper FD20, Amsterdam, Netherlands) was used to observe the process. At 6 weeks after surgery, the extent of disc degeneration was measured using a magnetic resonance imaging (MRI) system (MAGNETOM Verio 3.0T, Siemens AG, Erlangen, Germany). Four blinded investigators used the Pfirrmann classification system to classify disc images into 5 grades[18].

A rat IDD model was established as described above. The difference was in needle size, and a 20-gauge sterile syringe needle was used. MRI was performed to confirm that the degeneration model had been successfully established before and 4 weeks after surgery.

Then, animals were euthanized by 2.5% Avertine (50 ml/kg, ip), and tail samples were harvested. The proximal and distal adjacent intervertebral discs were used as blank controls.

H&E staining and safranin O-fast green (SO&FG) staining

Human nucleus pulposus (NP) tissue slices were obtained from Tongde Hospital, and hematoxylin and eosin (H&E) staining was performed. The histologic degeneration score (HDS) was assessed according to the clinically modified parameters of disc degeneration[19].

Mouse and rat Co4-7 coccygeal discs were fixed in 4% paraformaldehyde for 48 h, decalcified in fast decalcifying solution (Preserve, Zhuo Ding, Beijing) for 72 h, embedded in paraffin and cut into 5 μm sections. Then, the sections were deparaffinized and dehydrated for histological analysis, and hematoxylin and eosin (H&E), and safranin O-fast green (SO&FG) staining were performed separately on consecutive tissue sections. Finally, the slices were dehydrated, cleared, and sealed. Images were obtained using a SLIDEVIEW VS200 workstation (Olympus, China). HDS was determined according to the histological characteristics of the nucleus pulposus following the standardized histopathology scoring system ranging from 0 for no degeneration to 2 for severe degeneration[20], based on morphology and cellularity of NP and AF, NP-AF border, and endplate.

Immunohistochemistry (IHC) assays

The sections were deparaffinized and dehydrated as described for H&E staining. After that, endogenous peroxidase activity was quenched by treating the paraffin sections with 0.3% H_2O_2 for 10 min; antigen retrieval was performed with 10 mM citrate buffer (pH 6.0) for efficient epitope exposure; and nonspecific binding of antibodies was eliminated using blocking buffer (5% BSA in PBS) for 10 min. Afterward, the sections were incubated with primary antibodies, phospho-SAPK/JNK (Thr183/Tyr185) (G9) mouse mAb (CST, #9255, 1:50) or anti-NLRP3/NALP3 mAb (cryo-2) (Adipogen, AG-20B-0014.1:200) at 4 °C overnight, followed by incubation with biotinylated IgG and streptavidin-horseradish peroxidase for 30 min at room temperature, after which DAB (2 mg/ml) was used to visualize the immunoreactivity. Finally, the sections were counterstained with hematoxylin and mounted. Images were obtained using a SLIDEVIEW VS200 workstation (Olympus, China). Analyzing IHC images using ImageJ, particularly with the Fuji plugin, selecting 5 views from one slide, and quantifying every view.

Enzyme-linked immunosorbent assay (ELISA)

Human serum from the patients, the cell culture supernatant, and homogenized human NP tissue supernatant were used to determine the levels of inflammatory cytokines. An enzyme-linked immunosorbent assay (ELISA) kit for interleukin-1b (IL-1β, DY401, interleukin-6 (IL-6, DY406), and tumor necrosis factor-α (TNF-α, DY410) was purchased from R&D Systems (Minneapolis, USA). An IL-18 ELISA kit (SEK50073) was purchased from Sino Biological (Beijing, China). All procedures were carried out according to the manufacturer's instructions. The samples were prepared and analyzed in technical duplicates.

Western blot

Proteins were extracted from the cells and tissue samples by using cold radioimmunoprecipitation assay (RIPA) lysis buffer (including 1% protease inhibitor cocktail (Roche Diagnostics, USA), 2% PMSF (Millipore Sigma) and 1× PhosSTOP (Roche Diagnostics, USA), and the samples were incubated for 10 min at 12,000 rpm and 4 °C. Later, the supernatant was collected, and the protein concentration was evaluated using the Bradford assay (Thermo Fisher Scientific, USA). Approximately 50 μg of protein was prepared for western blot analysis. 5× loading buffer (Beyotime, Beijing, China) was added to the protein sample, which was subsequently denatured for 5 min at 100 °C. Briefly, 10% sodium dodecyl sulfate polyacrylamide (SDS) gel electrophoresis was used to separate the proteins, which were subsequently transferred to a nitrocellulose membrane (PALL BioTrace, # 66485, USA) for 70 to 90 min at 300 mA (Mini-protein II System, Bio-Rad, USA). The membrane was blocked with Tris-buffered saline supplemented with 5% BSA for 1 h at room temperature. The membranes were incubated with primary antibodies diluted 1:1000 or 1:5000 in primary antibody diluent solution at 4 °C overnight. Primary antibodies included anti-NLRP3 (AG-20B-0014, Adipogen, South Korea, 1:1000), anti-phospho-SAPK/JNK (#9255, CST, USA, 1:1000), anti-PDE4B (PD4-201AP, FabGennix, USA, 1:1000) and anti-GAPDH (db106, Daigbio, China, 1:5000). After five washes with 1× TBST, the membranes were incubated with fluorescent conjugated secondary antibodies (IRDye 800CW goat anti-rabbit; IRDye 680CW goat anti-mouse; LI-COR Biosciences, 1:5000) for 1.5 h at room temperature. Immunoblots were scanned and quantified with an Odyssey imaging analysis system (Image Studio Ver 5.2, LI-COR Biosciences). GAPDH was used as the protein loading control.

Quantification and statistical analysis

The data are presented as the means ± SEMs. All the experiments were performed as at least three independent experiments. The data were analyzed with One-way or Two-way ANOVA and Student's t test where appropriate. All the statistical analyses were performed with GraphPad Prism 9.0 software. $p < 0.05$ was considered to indicate statistical significance.

Results

PDE4B/NLRP3 expression increases in the NP tissues of IDD patients, accompanied by JNK activation

To further validate the expression of PDE4B and NLRP3 in the process of IDD, we collected human NPs with different Pfirrmann grades from the MR images (Fig. 1A). H&E staining suggested that more chondrocyte proliferation occurred in patients with higher grades (Fig. 1B). To further confirm the relationship between IDD and JNK activation, we collected a total of 12 samples from patients with different Pfirrmann grades from the MR images. Immunohistochemical staining revealed a greater proportion of p-Jun N-terminal kinase (p-JNK) positive cells and NLRP3 positive cells in sections from the Grade IV/V group than that in sections

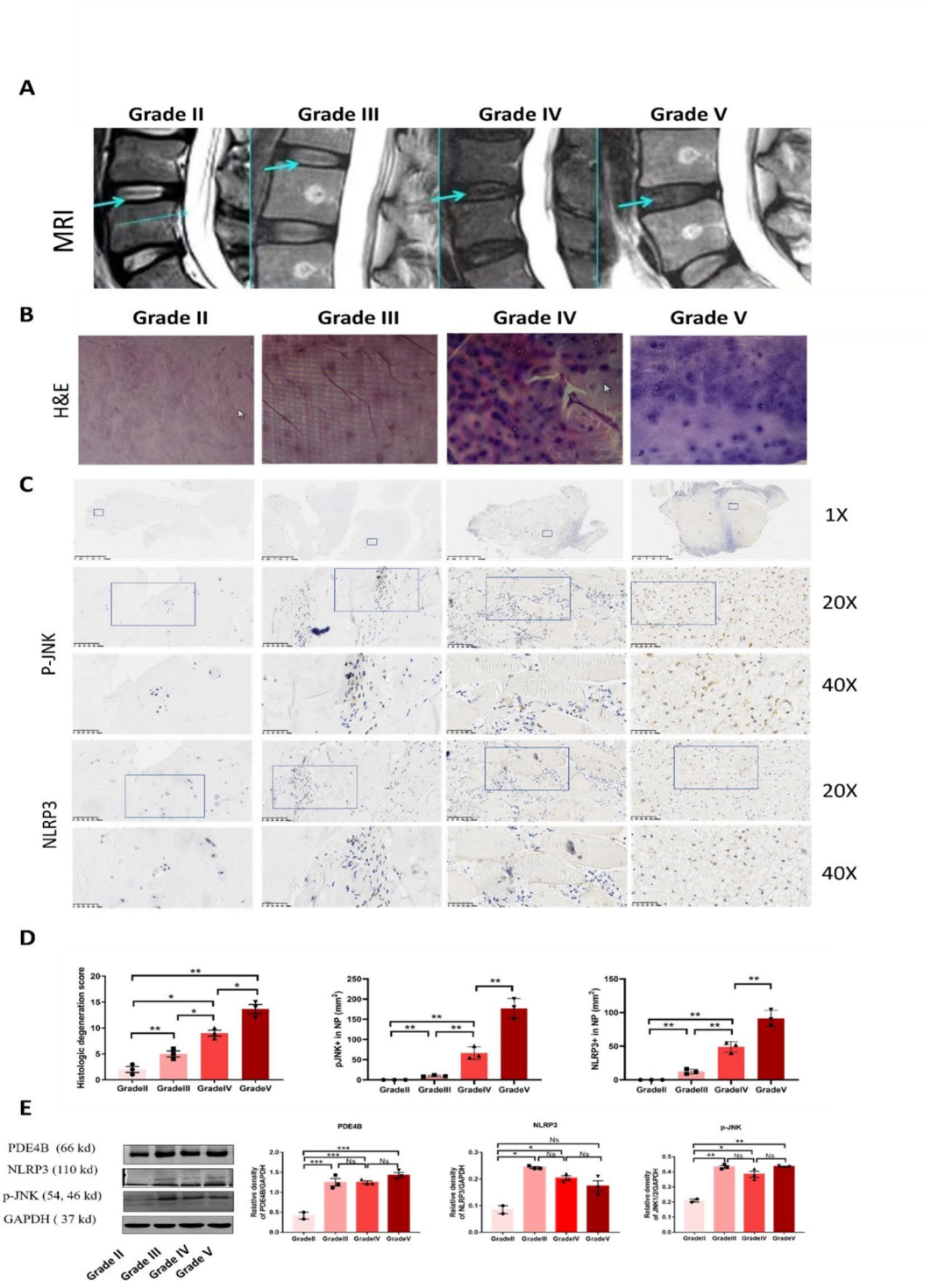

Fig. 1 . PDE4B/NLRP3 expression increases in the NP tissues of IDD patients accompanied by JNK activation. (**A**) Typical MRI schematic diagram of IDD patients with different degrees of lesion. (**B**) Representative images of HE staining of IDD patients with different degrees of lesion. (**C**) Representative IHC staining of phosphorylated JNK and NLRP3 in nucleus pulposus tissue from Grade II/III and Grade IV/V IDD patients. The magnifications are 1×, 20×, and 40×. (**D**) Quantification of p-JNK-positive cells and NLRP3-positive cells in human NP tissues from Grade II/III and Grade IV/V patients. (**E**) Representative western blot images of PDE4B, NLRP3, and phosphorylated JNK detected in NP tissues from IDD patients and quantitative analysis. Statistical differences between groups were analyzed by one-way ANOVA. The data shown are the means ± SEMs. The biological replicates are 3. * $p < 0.05$, ** $p < 0.01$, *** $p < 0.001$.

from the Grade II/III group (Fig. 1C&D), indicating a negative relationship between JNK activation and IDD severity. To investigate the effects of PDE4B, NLRP3 and JNK activation in the process of IDD, the protein levels were measured by western blot in human samples from patients with different degrees of IDD. Western blot analysis revealed that the PDE4B, NLRP3 and p-JNK protein levels increased as the NP lesion size increased (Fig. 1E). These results demonstrated that the levels of pJNK and NLRP3 in human NP tissues were increased following PDE4B signaling during IDD progression.

Additionally, according to the results of ELISA analysis, the cytokine levels of IL-1β, TNF-α, IL-6 and IL-18 in the serum of IDD patients with different degrees did not significantly change according to the degree of IDD (Fig. 2A). However, the cytokine levels of IL-1β and IL-18 in the nucleus pulposus significantly changed in a manner dependent on the degree of IDD (Fig. 2B), while IL-1β and IL-18 are related to NLRP3. These findings indicate that the inflammatory factor level in the serum of patients with intervertebral disc degeneration (IDD) is not strongly correlated with the severity of IDD. In contrast, the inflammatory factor in the NP is strongly associated with IDD severity.

PDE4B upregulates the activation of JNK/NLRP3 and the release of inflammatory cytokines in primary human NP cells

To determine whether PDE4B plays a role in activating NLRP3 and p-JNK in NP cells, NP cells were transfected with the vector control EGFP or EGFP-PDE4B plasmid, and the protein levels of PDE4B, NLRP3 and p-JNK were measured. As expected, the PDE4B overexpression plasmid increased PDE4B, NLRP3 and p-JNK expression (Fig. 3A**&B**) and increased the production of the inflammatory cytokines IL-1β, TNF-α, IL-6 and IL-18 (Fig. 3C). Taken together, these data suggested that overexpression of PDE4B enhanced the protein expression of NLRP3 and p-JNK and cytokine levels in NP cells. Additionally, to evaluate the expression of PDE4B, NLRP3 and p-JNK in NP cells, NP cells were treated with LPS (10 ng/ml) plus nigericin (10 μM). The results suggested that the expression of PDE4B and NLRP3 and the phosphorylation of JNK can be induced by LPS plus nigericin. After the transfection of PDE4B-Si in NP cells, the expression of NLRP3 and p-JNK was suppressed compared with that in the LPS plus nigericin group (Fig. 3D **&** **E**). ELISA analysis revealed significant decreases in the extracellular IL-1β, TNF-α, IL-6 and IL-18 levels in NP cells after transfection with PDE4B-Si (Fig. 3F). These data collectively suggested that PDE4B regulate NLRP3 expression, IL-1β production and JNK signaling.

PDE4B deleted mice are more resistant to the degeneration of intervertebral disc

To further validate the effect of PDE4B on NP tissue *in vivo*, we induced puncture-induced IDD or performed sham surgery on wild-type (WT) mice or PDE4B KO mice (the WT sham group, KO sham group, WT IDD group, and KO IDD group). After 6 weeks, MRI was performed to evaluate the degree of disc degeneration. The results revealed that the degree of NP degeneration in the KO IDD group was significantly lower than that in the control group, suggesting that PDE4B deletion could reduce the degeneration of nucleus pulposus cells in intervertebral disc tissue (Fig. 4A). To further investigate the changes in IDD, mouse intervertebral discs were histologically stained. All groups were subjected to safranin O-fast green staining and histological grading (Fig. 4B). The AF arrangement in the WT puncture group was disrupted, the structure of the semi annular concentric circle was disrupted, and the extent of nucleus pulposus fibrosis was more severe. The AF in the

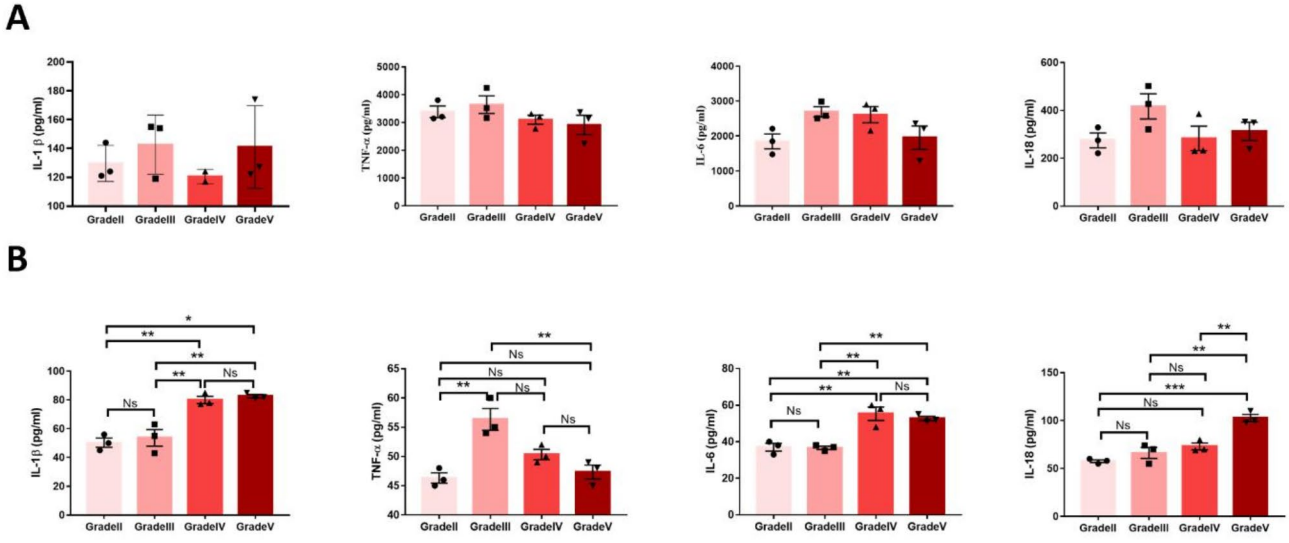

Fig. 2. The expression of inflammatory cytokines in the serum and nucleus pulposus tissue of IDD patients. (**A**) Inflammatory cytokines such as IL-β, TNF-α, IL-6, and IL-18 in the peripheral blood serum of patients with different degrees of lesions. (**B**) Inflammatory cytokines such as IL-β, TNF-α, IL-6, and IL-18 in the NP tissue of patients with different degrees of lesions. Statistical differences between groups were analyzed by one-way ANOVA. The data shown are the means ± SEMs.The biological replicates are 3. * $p < 0.05$, ** $p < 0.01$, *** $p < 0.001$.

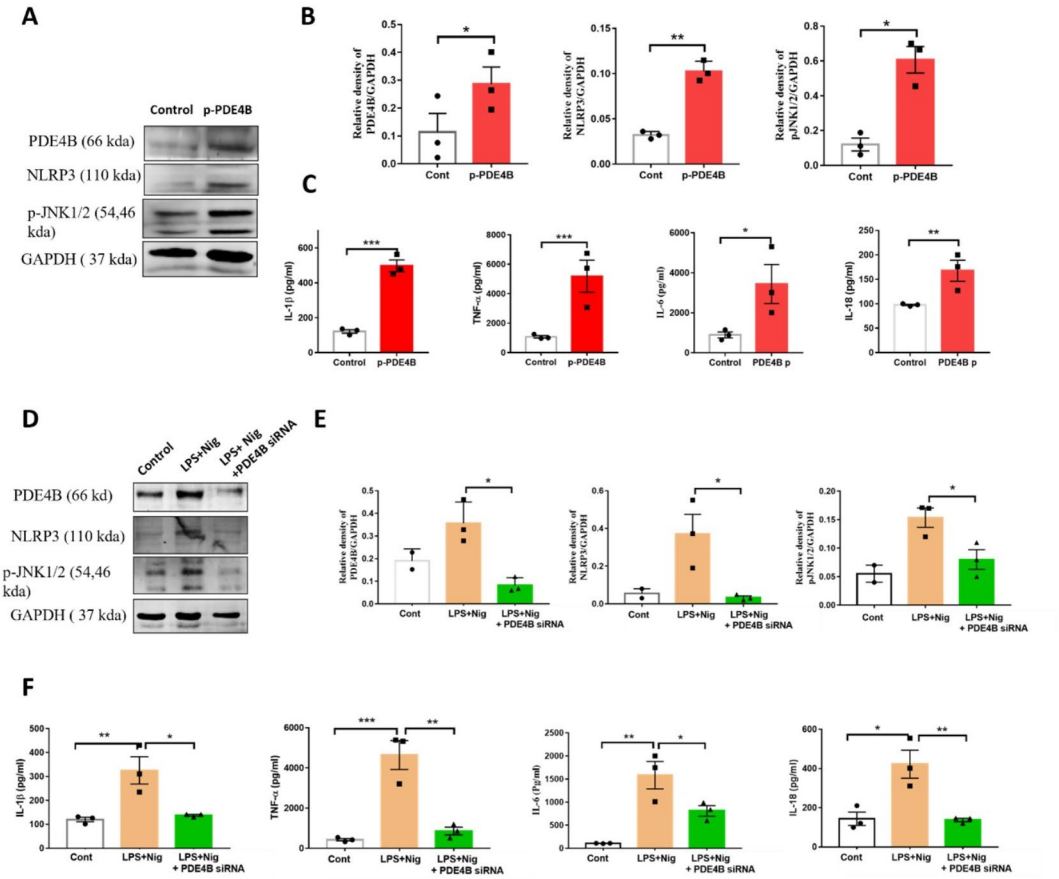

Fig. 3. PDE4B regulates the expression of JNK/NLRP3 and the release of inflammatory cytokines in primary human NP cells. (**A**-**C**) Overexpression of PDE4B in primary NP cells can induce NLRP3 activation and JNK phosphorylation. (**A**) Representative WB diagram. (**B**) Quantitative analysis of the WB results. (**C**) Changes in the inflammatory cytokines ILβ, TNF-α, IL-6, and IL-18 in the cell culture supernatant of primary NP cells overexpressing PDE4B. (**D**-**F**) Transfection of PDE4B siRNA into primary NP cells can completely reverse the activation of NLRP3 and JNK phosphorylation induced by lipopolysaccharide (LPS) combined with nigericin (Nig) (a NLRP3 activator). (**D**) Representative WB; (**E**) Quantitative analysis of the WB data; (**F**) Changes in the inflammatory cytokines IL-β, TNF-α, IL-6, and IL-18 in the cell culture supernatant of PDE4B siRNA-transfected primary NP cells. Statistical differences between groups were analyzed by two-way ANOVA. The data shown are the means ± SEMs. The biological replicates are 3. * $p < 0.05$, ** $p < 0.01$, ***$p < 0.001$.

PDE4B KO puncture group was still neat, vacuolar cells appeared in the NP, and fibrosis also occurred, however, the degree of degeneration was lesser in the PDE4B KO mice than that in the WT mice. These results also indicated that PDE4B deficiency could relieve the degeneration of NP in intervertebral disc tissue.

To further investigate JNK activation in the IDD model, IHC staining of phosphorylated JNK in mouse intervertebral discs was performed. Consistent with the MRI and histological data, the phosphorylation of JNK was also more severe in the WT IDD mice than that in the PDE4B KO mice (Fig. 4C). These results demonstrated that JNK was associated with PDE4B-mediated nucleus pulposus degeneration.

PDE4 inhibitor effectively alleviates the degenerative phenotype in a puncture-induced IDD rat model

To determine whether our findings have potential translational significance, we generated a rat tail puncture model or performed sham surgery followed by intraperitoneal injection of roflumilast. These results suggested that the PDE4 inhibitor could restore NP tissues. MRI showed that 4 weeks after puncture, the degree of degeneration of the rat IVDs significantly increased, while treatment with roflumilast partially restored the Pfirrmann grade induced by needle puncture (Fig. 5A**&C**). H&E and SO&FG staining revealed that needle puncture led to a reduced number of NP cells, accompanied by disorganized AF lamellae and collapsed cartilage endplates. Unsurprisingly, roflumilast treatment successfully ameliorated the histological damage induced by needle puncture (Fig. 5B**&D**). Taken together, our results further demonstrated the role of the PDE4B in regulating IVD homeostasis and confirmed the therapeutic effects of PDE4B inhibition on IDD *in vivo*.

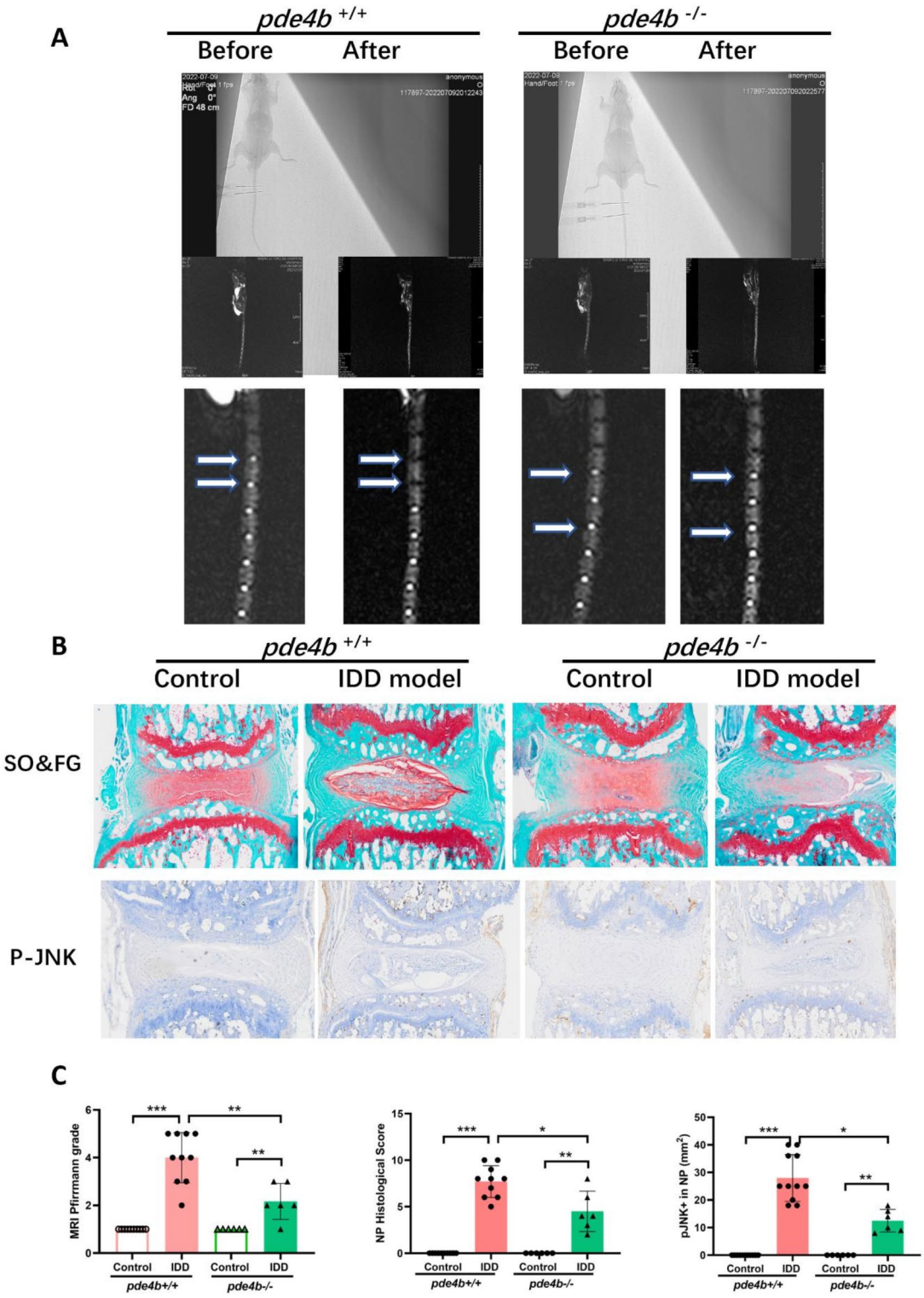

Fig. 4. *Pde4b* gene knockout inhibits the progression of IDD lesions in mice model. (**A**) Representative magnetic resonance image of PDE4B KO and WT mice before and after modeling. The white arrow indicates the needle puncture site. (**B**) Representative pathological images of intervertebral disc tissue from PDE4B KO and WT mice stained with safranin and fast green and immunohistochemically detected phosphorylated JNK. (**C**) Typical MRI schematic diagram, histological degeneration score and quantification of p-JNK positive cells in NP tissues. Statistical differences between groups were analyzed by two-way ANOVA. The data shown are the means ± SEMs. The biological replicates are 3–5. * $p < 0.05$, ** $p < 0.01$, *** $p < 0.001$.

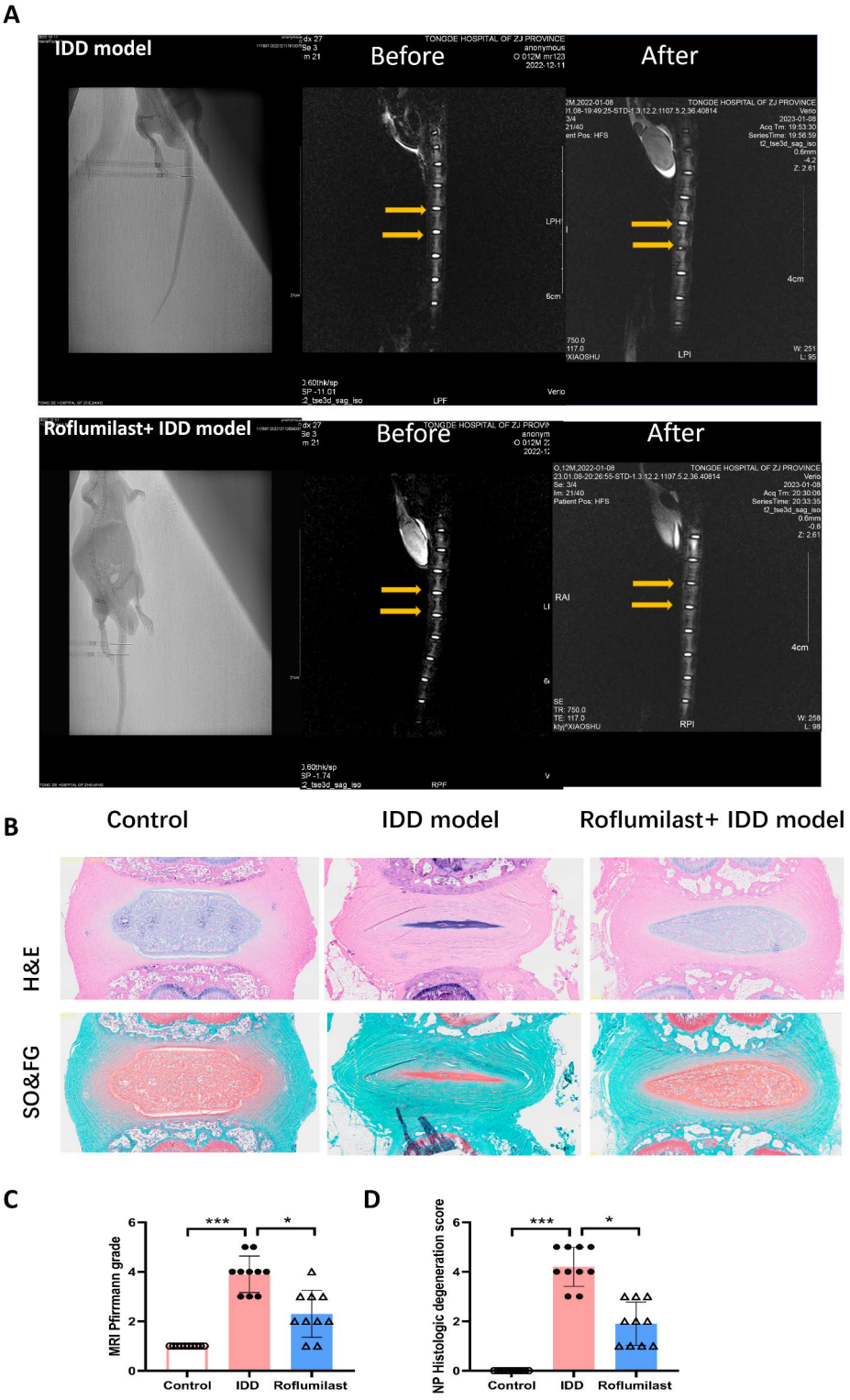

Fig. 5. PDE4 inhibitor roflumilast reduce the progression of IDD lesions in rat model. (**A**) Representative MR images of IDD model and roflumilast-treated IDD model before and after modeling. The orange arrow indicates the needle puncture site. (**B**) Representative pathological images of intervertebral disc tissue from control, IDD model and roflumilast-treated IDD model stained with safranine and fast green and stained with H&E. (**C**) MRI degeneration score of control, IDD model and roflumilast-treated IDD model. (**D**) NP histologic degeneration score of control, IDD model and roflumilast-treated IDD model. Statistical differences between groups were analyzed by two-way ANOVA. The data shown are the means ± SEMs. The biological replicates are 5. * $p < 0.05$, ** $p < 0.01$, *** $p < 0.001$.

Discussion

In this study, we firstly explored the involvement of PDE4B in the development of IDD and identified PDE4B as a target in the nucleus pulposus. The expression of PDE4B in the lung was reported to increase in pulmonary diseases such as COPD, asthma, lung fibrosis, and acute lung injury[11]. Furthermore, in an animal model, PDE4B knockout resulted in stronger anti-inflammatory phenotypes than did wild-type control PDE4B in acute lung injury, indicating the potential beneficial effect of PDE4B in inflammatory disorders[21]. However, no study has comprehensively investigated the role of PDE4B in the development of IDD. Our study is the first to show that the expression of PDE4B is correlated with IDD severity and that PDE4B inhibition can protect NP cells.

PDE4B is a main subtype of PDE4 expressed in immune cells and the central nervous system and plays an important role in inflammation, the immune response, and tumor regulation[12]. Studies on the pathological mechanism of IDD have revealed many different cell death modes, such as apoptosis, autophagy, pyroptosis, and ferroptosis, in the process of IDD. Pyroptosis is closely related to the inflammatory response. Many studies have shown that the caspase-1-mediated pyrosis pathway plays a crucial role in IDD, and significant activation of the NLRP3 inflammasome has been observed in NP tissues collected from patients with disc degeneration compared to those collected from patients with idiopathic scoliosis[5–7]. These studies suggested that pyroptosis pathway mediated by the NLRP3 inflammasome is an important feature of nucleus pulposus degeneration. In our studies, we further confirmed that PDE4B can regulate NLRP3 in NP degeneration. These results are consistent with our previous work in alveolar macrophages showing that PDE4B can activate NLRP3[21].

The stress response pathway involving the JNK signaling pathway is also closely related to the regulation of pyroptosis. The JNK/NLRP3 signaling pathway has been reported to be involved in *Listeria monocytogenes*-induced sepsis[22] and the cognitive impairment induced by surgical stress[23]. Many studies have suggested that JNK activation is involved in the apoptosis of NP cells[17]. However, whether the JNK/NLRP3 signaling pathway is involved in the pathogenesis of IDD has still been poorly studied. Therefore, in this study, we firstly provided evidence that JNK/NLRP3 mediates IDD progression. In the human degenerated nucleus pulposus, activated JNK was highly consistent with NLRP3. Moreover, PDE4B induced JNK and NLRP3 activation, while the deletion of PDE4B decreased JNK and NLRP3 activation.

In addition, our study demonstrated that overexpression of PDE4B can effectively promote pyroptosis in NP cells. We also validated the therapeutic effect of a PDE4B inhibitor on IDD in a rat tail needle puncture model. The above-mentioned *in vitro* and *in vivo* data all indicated that the inhibition of PDE4B could be a promising therapeutic target for IDD. For a long time, members of the PDE4 family have attracted much attention in the field of neurodegeneration[24]. Few studies focused on IDD. Our study showed that PDE4B plays a key role in IDD progression and that promoting the expression of PDE4B can significantly induce JNK/NLRP3 activation in NP cells, ultimately accelerating the occurrence and progression of IDD. Since PDE4B is the known cAMP-degrading enzyme and located primarily in immune cells, the crucial role of PDE4B in maintaining the nucleus pulposus should be furtherly investigated. Inhibition of PDE4B can rescue against inflammatory disease in lung and other organs, so therapeutically targeting PDE4B is of interest.

PDE4 is also crucial in the hormonal regulation of bone metabolism, chronic PDE4 inhibition may influence bone remodeling processes. For example, rolipram doses of 0.1–0.6 mg/kg prevented ovariectomy-induced bone loss, while 1 mg/kg restored lost bone in the tibia, femur, and lumbar vertebrae. The beneficial effects were attributed to maintained elevated bone formation at the trabecular surface and increased formation at the cortical periosteal surface. Rolipram also reduced bone turnover at the trabecular and endocortical surfaces. In addition, rolipram treatment increased body and muscle weights compared to the vehicle-treated ovariectomy rats[25], and enhanced the bone-inducing effects of BMP-2 in mesenchymal cells, increasing responsiveness to BMP-2, which indicate a potential use for PDE4 inhibitors in promoting rhBMP-dependent bone repair[26]. Cilomilast, a second-generation PDE4 inhibitor, could enhance the osteoblastic differentiation of mesenchymal stem cells, equally well as rolipram in primary cultured MSCs[27]. It suggested that a selective PDE4 inhibitor may be used for the treatment of established osteoporosis. Autosomal Dominant Osteopetrosis type II (ADO2), which is missense mutations in the chloride channel 7, leading to impaired osteoclastic bone resorption[28]. Recent study suggested that rolipram and roflumilast rescues cAMP levels and osteoclast dysfunction in ADO2, suggested the potential of PDE4 inhibitor for ADO2[29]. Another clinical trial to study the efficacy and safety of an oral phosphodiesterase 4 inhibitor, apremilast in ankylosing spondylitis, the results suggested that apremilast was associated with numerically greater improvement from baseline for all clinical assessments compared with placebo, and serum RANKL and RANKL: osteoprotegrin ratio and plasma sclerostin were statistically significant decreases [30]. So, all those data suggested that PDE4 inhibition could be benefit for bone formation and repair.

This study has several limitations. First, due to the limitation of mouse volume, it was almost impossible to obtain the nucleus pulposus from the vertebral bodies of the mice to perform protein and PCR analyses. Additional studies using large animals, such as dogs[31], goats[32], monkeys[33], and baboons[34] could provide further insights. Second, in contrast to conditional knockout mice, *pde4b* global knockout mice cannot rule out the influence of complex phenotypes, and may introduce systemic effects unrelated to NP-specific pathology. Third, we cannot rule out that intraperitoneal injection of the PDE4 inhibitor roflumilast may affect the function of NP tissue by altering the secretome or through other unknown mechanisms. Fourth, we didn't evaluate the potential side effects or off-target effects of PDE4 inhibition, particularly in the context of long-term systemic administration, there are many known side effects of rofumilast, such as nausea, diarrhea are common side effects. So, further studies are needed to explore the detailed mechanism of action of roflumilast *in vivo*. Moreover, PDE4B also regulate other pathway, such as NF-κB, a classical NLRP3 activation pathway. In fact, we have checked it in lung or macrophage, we found that PDE4B knockout can significantly decrease the phosphorylation of p65, so we proposed that p65 also involve in the NLRP3 activation of NP cells. So, the molecular mechanism of PDE4B-induced JNK/NLRP3 activation in NP cells is worthy of further investigation.

In summary, our study reveals a novel target and molecular mechanism of disc degeneration. Our results first demonstrated that PDE4B increases JNK/NLRP3 activation in NP cells, contributing to the subsequent occurrence of IDD. Finally, we evaluated the effectiveness of *pde4b* deletion and PDE4 inhibition. Overall, our study provides new insights into the occurrence and development of IDD and offers promising therapeutic approaches for treating IDD.

Data availability

The data used and analyzed in the current study are available from the corresponding author upon reasonable request.

Received: 5 July 2024; Accepted: 23 January 2025
Published online: 17 February 2025

References

1. Tang, S. N. et al. In vivo mouse intervertebral disc degeneration models and their utility as translational models of clinical discogenic back Pain: a comparative review. *Front. Pain Res. (Lausanne)*. **3**, 894651 (2022).
2. Oichi, T., Taniguchi, Y., Oshima, Y., Tanaka, S. & Saito, T. Pathomechanism of intervertebral disc degeneration. *JOR Spine*. **3**, e1076 (2020).
3. Zhao, H. et al. Effects of bone cement on intervertebral disc degeneration. *Exp. Ther. Med.* **7**, 963–969 (2014).
4. Hrabalek, L., Adamus, M., Wanek, T., Machac, J. & Tucek, P. Surgical complications of the anterior approach to the L5/S1 intervertebral disc. *Biomed. Pap Med. Fac. Univ. Palacky Olomouc Czech Repub.* **156**, 354–358 (2012).
5. Tang, P. et al. The NLRP3/Caspase-1/Interleukin-1beta Axis is active in human lumbar cartilaginous endplate degeneration. *Clin. Orthop. Relat. Res.* **474**, 1818–1826 (2016).
6. Chao-Yang, G., Peng, C. & Hai-Hong, Z. Roles of NLRP3 inflammasome in intervertebral disc degeneration. *Osteoarthr. Cartil.* **29**, 793–801 (2021).
7. Chen, Z. H. et al. Enhanced NLRP3, caspase-1, and IL- 1beta levels in degenerate human intervertebral disc and their association with the grades of disc degeneration. *Anat. Rec (Hoboken)*. **298**, 720–726 (2015).
8. Sun, Y. et al. Piezo1 activates the NLRP3 inflammasome in nucleus pulposus cell-mediated by ca(2+)/NF-kappaB pathway. *Int. Immunopharmacol.* **85**, 106681 (2020).
9. He, D. et al. Propionibacterium acnes induces intervertebral disc degeneration by promoting nucleus pulposus cell pyroptosis via NLRP3-dependent pathway. *Biochem. Biophys. Res. Commun.* **526**, 772–779 (2020).
10. Tang, G. et al. Propionibacterium acnes Accelerates Intervertebral Disc Degeneration by Inducing Pyroptosis of Nucleus Pulposus Cells via the ROS-NLRP3 Pathway. Oxid Med Cell Longev 2021:4657014. (2021).
11. Liu, Z., Liu, M., Cao, Z., Qiu, P. & Song, G. Phosphodiesterase4 inhibitors: a review of current developments (2013–2021). *Expert Opin. Ther. Pat.* **32**, 261–278 (2022).
12. Bailly, C. The potential value of amlexanox in the treatment of cancer: molecular targets and therapeutic perspectives. *Biochem. Pharmacol.* **197**, 114895 (2022).
13. Abou Saleh, L. et al. Ablation of PDE4B protects from Pseudomonas aeruginosa-induced acute lung injury in mice by ameliorating the cytostorm and associated hypothermia. *Faseb j.* **35**, e21797 (2021).
14. Karam, S. et al. Cardiac overexpression of PDE4B blunts β-Adrenergic response and maladaptive remodeling in Heart failure. *Circulation* **142**, 161–174 (2020).
15. Myers, S. A. et al. Following spinal cord injury, PDE4B drives an acute, local inflammatory response and a chronic, systemic response exacerbated by gut dysbiosis and endotoxemia. *Neurobiol. Dis.* **124**, 353–363 (2019).
16. Shen, S. et al. circPDE4B prevents articular cartilage degeneration and promotes repair by acting as a scaffold for RIC8A and MID1. Annals of the rheumatic diseases 2021, **80**:1209–1219 .
17. Das, U. N. Bioactive lipids in intervertebral disc degeneration and its therapeutic implications. *Biosci. Rep.* 39. (2019).
18. Pfirrmann, C. W., Metzdorf, A., Zanetti, M., Hodler, J. & Boos, N. Magnetic resonance classification of lumbar intervertebral disc degeneration. *Spine (Phila Pa. 1976)*. **26**, 1873–1878 (2001).
19. Weiler, C. et al. Histological analysis of surgical lumbar intervertebral disc tissue provides evidence for an association between disc degeneration and increased body mass index. *BMC Res. Notes*. **4**, 497 (2011).
20. Lai, A. et al. Development of a standardized histopathology scoring system for intervertebral disc degeneration in rat models: an initiative of the ORS spine section. *JOR Spine*. **4**, e1150 (2021).
21. Dhar, R. et al. Phosphodiesterase 4B is required for NLRP3 inflammasome activation by positive feedback with Nrf2 in the early phase of LPS- induced acute lung injury. *Free Radic Biol. Med.* **176**, 378–391 (2021).
22. Gao, A. et al. Mst1/2-ALK promotes NLRP3 inflammasome activation and cell apoptosis during Listeria monocytogenes infection. *J. Microbiol.* **59**, 681–692 (2021).
23. He, J. et al. JNK inhibition alleviates delayed neurocognitive recovery after surgery by limiting microglia pyroptosis. *Int. Immunopharmacol.* **99**, 107962 (2021).
24. Ribaudo, G., Ongaro, A., Zagotto, G., Memo, M. & Gianoncelli, A. Therapeutic potential of phosphodiesterase inhibitors against Neurodegeneration: the perspective of the Medicinal chemist. *ACS Chem. Neurosci.* **11**, 1726–1739 (2020).
25. Yao, W. et al. Rolipram, a phosphodiesterase 4 inhibitor, prevented cancellous and cortical bone loss by inhibiting endosteal bone resorption and maintaining the elevated periosteal bone formation in adult ovariectomized rats. *J. Musculoskelet. Neuronal Interact.* **7**, 119–130 (2007).
26. Horiuchi, H. et al. Effect of phosphodiesterase inhibitor-4, rolipram, on new bone formations by recombinant human bone morphogenetic protein-2. *Bone* **30**, 589–593 (2002).
27. Munisso, M. C., Kang, J. H., Tsurufuji, M. & Yamaoka, T. Cilomilast enhances osteoblast differentiation of mesenchymal stem cells and bone formation induced by bone morphogenetic protein 2. *Biochimie* **94**, 2360–2365 (2012).
28. Waguespack, S. G. et al. Chloride channel 7 (ClCN7) gene mutations and autosomal dominant osteopetrosis, type II. *J. Bone Miner. Res.* **18**(8), 1513–1518 https://doi.org/10.1359/jbmr.2003.18.8.1513 (2003).
29. Hong, J. M. et al.The PDE4 Inhibitors Roflumilast and Rolipram Rescue ADO2 Osteoclast Resorption Dysfunction. *Calcif Tissue Int.* **114**(4), 430–443 https://doi.org/10.1007/s00223-024-01191-7 (2003).
30. Pathan, E. et al. Efficacy and safety of apremilast, an oral phosphodiesterase 4 inhibitor, in ankylosing spondylitis. *Ann. Rheum. Dis.* **72**, 1475–1480 (2013).
31. Bergknut, N. et al. The dog as an animal model for intervertebral disc degeneration? *Spine (Phila Pa. 1976)*. **37**, 351–358 (2012).
32. Gullbrand, S. E. et al. A large animal model that recapitulates the spectrum of human intervertebral disc degeneration. *Osteoarthr. Cartil.* **25**, 146–156 (2017).
33. Longo, U. G., Ripalda, P., Denaro, V. & Forriol, F. Morphologic comparison of cervical, thoracic, lumbar intervertebral discs of cynomolgus monkey (Macaca fascicularis). *Eur. Spine J.* **15**, 1845–1851 (2006).

34. Platenberg, R. C., Hubbard, G. B., Ehler, W. J. & Hixson, C. J. Spontaneous disc degeneration in the baboon model: magnetic resonance imaging and histopathologic correlation. *J. Med. Primatol.* **30**, 268–272 (2001).

Acknowledgements
We are thankful for the technical support of Li Liu and Guifeng Xiao in the Core Facilities, at Zhejiang University School of Medicine.

Author contributions
Weixin Xu contributed to the methodology, investigation, and resources. Rana Dhar and KaiYue Li contributed to the methodology, investigation, writing, data analysis, and visualization. Danyang Zheng contributed to the clinical sample collection. Weiguo Ding, Bin Xu, Long Xing, Minxing He, Yuqing He, and Qi Peng contributed to the methodology and investigation. Huifang Tang contributed to conceptualization, supervision, and revision. All authors reviewed the manuscript.

Funding
Funded by the Basic Public Welfare Research Program of Zhejiang Province (China) (No. TGY24H060008), the Medical and Health Technology Plan of Zhejiang Province (China) (No. 2023KY078) and the Chinese Medicine Research Program of Zhejiang Province (China) (No: 2019ZB023).

Declarations

Consent for publication
Not applicable.

Competing interests
The authors declare no competing interests.

Ethics approval
was obtained from the Ethics Committee of Tongde Hospital of Zhejiang Province (No. 202122-088). Informed consent was obtained from all participants enrolled in this study. The study was conducted according to the Code of Ethics of the World Medical Association (Declaration of Helsinki). All animal procedures were approved by the Animal Care and Use Committee of Zhejiang University.

Accordance
We confirmed that all experiments in this study were performed in accordance with the relevant guidelines and regulations.

Arrive
All the procedure of the study is followed by the ARRIVE guidelines.

Additional information
Correspondence and requests for materials should be addressed to H.T.